161 (1982); G. Poste, *Cancer Treat. Rep.* **70**, 183 (1986); G. L. Nicholson, *Cancer Res.* **47**, 1473 (1987).
4. L. Foulds, *Neoplastic Development* (Academic Press, New York, 1975), vol. 2.
5. E. Otto, S. McCord, T. D. Tlsty, *J. Biol. Chem.* **264**, 3390 (1989).
6. T. D. Tlsty, B. H. Margolin, K. Lum, *Proc. Natl. Acad. Sci. U.S.A.* **86**, 9441 (1989).
7. T. D. Tlsty, *ibid.* **87**, 3132 (1990).
8. J. A. Wright *et al.*, *ibid.*, p. 1791.
9. E. J. Stanbridge, *Nature* **260**, 17 (1976).
10. _____ and J. Wilkinson, *Proc. Natl. Acad. Sci. U.S.A.* **75**, 1466 (1978).
11. W. F. Benedict, B. E. Weissman, C. Mark, E. J. Stanbridge, *Cancer Res.* **44**, 3471 (1984).
12. B. Weissman and E. J. Stanbridge, *Cytogenet. Cell Genet.* **28**, 227 (1980).
13. Diploid fibroblasts were hybridized with two tumorigenic cell lines of different tissue origin, a fibrosarcoma and a carcinoma. The progeny were extremely stable with a minimal loss of chromosomes after fusion (*9, 11*). The tumorigenicity of these hybrids was initially suppressed but, upon chromosome loss, was reexpressed (*11*). We verified that these hybrids still contained the expected chromosome complement and proliferated in the indicated selective media [hypoxanthine, aminopterin, thymidine (HAT) plus 5×10^{-7} M ouabain or 5×10^{-5} M ouabain alone (*11*)]. Both tumorigenic and nontumorigenic hybrids grew at rates comparable to the parental cell lines.
14. G. R. Stark and G. M. Wahl, *Annu. Rev. Biochem.* **53**, 447 (1984); R. T. Schimke, *Cell* **37**, 705 (1984).
15. G. M. Wahl, R. A. Padget, G. R. Stark, *J. Biol. Chem.* **254**, 8679 (1979).
16. T. D. Tlsty, M. Sage, A. White, L. Livingstone, unpublished results.
17. Metaphase chromosomes were isolated from sensitive cells and resistant subclones and analyzed for CAD gene copy number with fluorescence in situ hybridization [B. J. Trask and J. L. Hamlin, *Genes Dev.* **3**, 1913 (1989)]. Slides were viewed with a Microphot FXA microscope (Nikon) equipped with filters for fluorescein and propidium iodide, B-2A and G-1B, respectively. Visualization was at ×100 magnification with the use of a Fluor 100X DL objective (Nikon). Increases in CAD gene copy number were observed in all PALA-resistant cell lines.
18. E. S. Srivatsan, W. F. Benedict, E. J. Stanbridge, *Cancer Res.* **46**, 6174 (1986).
19. P. J. Saxon, E. S. Srivatsan, E. J. Stanbridge, *EMBO J.* **5**, 3461 (1986).
20. A. R. Robbins and R. M. Baker, *Biochemistry* **16**, 5163 (1977).
21. O. M. Pereira-Smith and J. R. Smith, *Proc. Natl. Acad. Sci. U.S.A.* **85**, 6042 (1988).
22. P. Chen and B. E. Weissman, in *Carcinogenesis*, part D of *Mutation and the Environment*, M. L. Mendelsohn and R. Albertini, Eds. (Wiley-Liss, New York, 1990), pp. 13–20.
23. L. A. Liotta, P. S. Steeg, W. G. Stetler-Stevenson, *Cell* **64**, 327 (1991).
24. J. A. Boyd and J. C. Barrett, *Pharmacol. Ther.* **46**, 469 (1990).
25. C. J. Der and E. J. Stanbridge, *Cell* **15**, 1241 (1978).
26. We thank B. Weissman whose continued enthusiasm and support helped make this study possible. We also thank E. Stanbridge, J. Davidson, V. Stewart, S. Earp, B. Margolin, C. Walker, B. Emerson, L. Hartwell, and members of the laboratory for supplies, critical reading of the manuscript, and stimulating discussion. This paper is dedicated to Theodore Tlsty. Supported by a gift from Glaxo, Inc., to T.D.T.

28 October 1991; accepted 9 January 1992

Formation of Ion-Permeable Channels by Tumor Necrosis Factor–α

BRUCE L. KAGAN, RAE LYNN BALDWIN,* DAVID MUNOZ, BERNADINE J. WISNIESKI†

Tumor necrosis factor–α (TNF, cachectin), a protein secreted by activated macrophages, participates in inflammatory responses and in infectious and neoplastic disease states. The mechanisms by which TNF exerts cytotoxic, hormonal, and other specific effects are obscure. Structural studies of the TNF trimer have revealed a central pore-like region. Although several amino acid side chains appear to preclude an open channel, the ability of TNF to insert into lipid vesicles raised the possibility that opening might occur in a bilayer milieu. Acidification of TNF promoted conformational changes concordant with increased surface hydrophobicity and membrane insertion. Furthermore, TNF formed pH-dependent, voltage-dependent, ion-permeable channels in planar lipid bilayer membranes and increased the sodium permeability of human U937 histiocytic lymphoma cells. Thus, some of the physiological effects of TNF may be elicited through its intrinsic ion channel–forming activity.

THE PROTEIN TNF CAUSES HEMORrhagic necrosis of certain solid tumors and is responsible for the physiological manifestations of "endotoxic shock" and the wasting syndrome (cachexia) of chronic disease. It also participates in positive and negative growth regulation and has direct effects on a wide variety of cells (*1*). Although TNF typically acts to combat infection and cancer growth, it notably enhances human immunodeficiency virus replication (*2*) and has permeabilizing effects on the vascular endothelium that may actually contribute to cancer metastasis (*3*).

Mature TNF acts as a compact trimer (~51 kD); each subunit is an antiparallel β barrel (*4, 5*). A long channel extends down the central axis of threefold symmetry (*4, 5*). Despite the compactness of the trimeric structure and the occluded appearance of the midregion of the channel, the trimer interface may be somewhat plastic because the three monomeric subunits are not precisely superimposable (*5*). The ability of TNF to insert into membranes (*6*) and to dissociate in mild detergent (*7*) supports this concept of interface plasticity. TNF insertion into the hydrocarbon core of phospholipid bilayers increases with decreasing pH (*6*). Acidification (pH 5.3, 15 min) also increases the cancer cell–killing activity of TNF (*6, 8*) while reducing specific binding (*9*). Two studies with model membrane targets have shown that TNF can increase vesicle permeability to calcein (*10*). Moreover, several physiological studies suggest TNF alters membrane permeability. Thus, TNF causes a rapid decrease in the resting membrane potential of skeletal muscle cells (*11*), similar to that observed in the endotoxic shock syndrome (*12*); this activity could account for the increased sodium space and fluid retention that occurs in shock. TNF also induces oligodendrocyte necrosis, myelin dilatation, and periaxonal swelling similar to that induced by batrachotoxin (which opens Na^+ channels) (*13*). To determine whether TNF might itself be a channel-forming molecule, a hypothesis consonant with its channel-like structure and membrane insertion activity, we evaluated the effects of human recombinant TNF on planar phospholipid membranes.

Figure 1A shows the current response of a TNF-treated membrane to a series of graded voltage (v) steps. In the absence of TNF, the membrane conductance was ohmic and equal to ~10 pS (indistinguishable from zero in Fig. 1). After addition of TNF to a final concentration of 100 ng/ml, the membrane current I (and therefore conductance, $g = I/V$) remained nearly zero at small voltages (absolute values of $V < 40$ mV). The side to which TNF was added was taken as ground; hence, voltages correspond to the "cytoplasmic" voltage. At larger positive voltages ($V > 40$ mV), the current rose within seconds to a new, higher steady state, which was steeply dependent on the membrane voltage. When the polarity of the voltage was reversed, the conductance de-

B. L. Kagan and D. Munoz, Department of Psychiatry, Neuropsychiatric Institute, Brain Research Institute, School of Medicine, University of California, and West Los Angeles Veterans Affairs Medical Center, Los Angeles, CA 90024.
R. L. Baldwin and B. J. Wisnieski, Department of Microbiology and Molecular Genetics, Molecular Biology Institute and Jonsson Comprehensive Cancer Center, University of California, Los Angeles, CA 90024.

*Initiated this collaborative research effort. Current address: Department of Medicine, University of California, Irvine, CA 92717.
†To whom correspondence should be addressed.

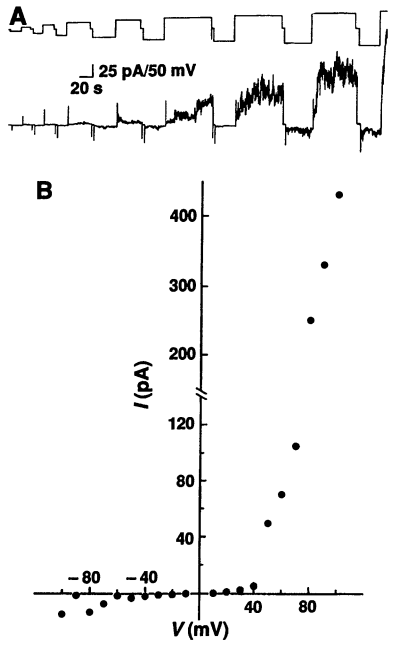

Fig. 1. Voltage-dependent currents induced by TNF in planar lipid bilayer membranes. (**A**) Membrane currents and voltages for a membrane treated with TNF (100 ng/ml). Top trace, a series of voltage pulses applied to the membrane beginning at ±10 mV and increasing in 10-mV increments to ±80 mV. Bottom trace, the current response of the membrane to the imposed voltage pulses. The linear spikes represent capacitative transients. At low voltages (±10 to ±30 mV), the current is nearly zero, which reflects the impermeability of lipid membranes to small ions in the aqueous phase. At higher voltages (V > +40 mV), the membrane current increases significantly and reaches a plateau within ~30 s. At negative voltages, the currents decay rapidly to a value close to that of an unmodified membrane. (**B**) The data from (A) plotted as a steady-state I-V curve. These experiments were conducted with human recombinant TNF and solvent-free membranes as described (*28*).

creased rapidly to ~0. Data from Fig. 1A are plotted as a steady-state current-voltage relation in Fig. 1B. The current remained ~0 at most negative voltages, whereas current values increased sharply at positive voltages. The conductance induced by TNF was due to formation of ion-permeable channels (Fig. 2). Observed single-channel conductances were heterogeneous, but could be grouped into two main classes, one centered at ~5 to 10 pS (Fig. 2A), and a second, larger class ranging from ~100 to 1000 pS (Fig. 2B). The most frequently observed event was 5 pS (Fig. 2C). Although channels can occasionally form at pH 7.2, channel formation was enhanced by lowering the pH of the aqueous phase containing TNF (Fig. 2D). The channel activities of diphtheria, tetanus, and botulinus toxins have a similar pH dependence (*14*). The enhancement of TNF cytotoxicity effected by pulsing target cancer cells with medium of pH 5.3 (*6, 8*) suggests that channel formation is involved in the TNF cytotoxic pathway. TNF channels exhibit preferential permeability for cations over anions, but not absolutely so. In a tenfold concentration gradient of NaCl, a TNF-treated membrane showed a reversal potential of ~25 to 30 mV (dilute side positive; an ideally cation-selective channel would give a reversal potential of ~51 mV).

The following data support the notion that channel formation is intrinsic to TNF. First, in the absence of added TNF, no channel activity was observed. Second, two separate, highly purified preparations of TNF (recombinant human TNF and natural human TNF) produced similar channel activity. Third, boiling TNF for 5 min, which eliminates biological activity, also eliminated channel-forming activity. Fourth, channel activity was enhanced by low pH. This is consistent with reports showing that membrane insertion (*6*) and permeabilization (*10*) increase at low pH. Although our results appear to conflict with others in which TNF had no effect on lipid membranes (*15*), those experiments were not performed in the presence of a pH gradient, a requirement for optimal TNF channel activity that is highly reminiscent of findings with diphtheria toxin (*14*). The bilayer lipid composition was also different.

Next, we asked whether the formation of Na^+-permeable TNF channels in lipid bilayers was correlated with an ability to alter the Na^+ permeability of target cancer cells (Fig. 3). Addition of TNF to human U937 histiocytic lymphoma cells increased $^{22}Na^+$ uptake by 100 to 300%, in the presence or absence of ouabain. The simplest explanation for this enhanced Na^+ uptake is a direct permeabilization of the target cell membrane by TNF. Na^+ uptake was consistent with the amount of channel activity seen in planar membranes at neutral pH. The aqueous space between macrophages, which secrete TNF, and their substrate has been determined to have a pH of 3.6 to 3.7 (*16*). Thus, the potential for substantial changes in intracellular free Na^+ concentrations ex-

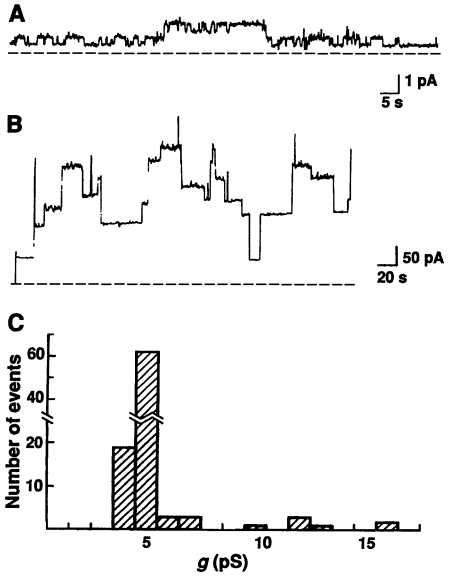

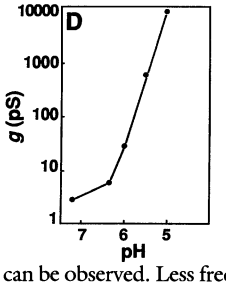

Fig. 2. Single-channel currents induced by TNF in lipid bilayer membranes. (**A**) The current through a membrane (*25*) held at +80 mV (dashed line indicates I = 0). Numerous fluctuations of the current, corresponding to a conductance of ~5 pS, can be observed. Less frequently, larger and smaller fluctuations can be seen. These fluctuations appear to represent the opening and closing of single ion-permeable channels in the membranes. (**B**) At later times (> 30 min) after TNF addition, large current fluctuations can be observed (dashed line indicates I = 0). These fluctuations are widely dispersed in size and may represent aggregation of TNF trimers in the membrane (*29*). (**C**) A frequency histogram of the current jumps shown in (A); 5 pS is the most frequently observed event. (**D**) Effect of pH on the ion-channel activity of TNF. The membrane (*30*) was held at +100 mV for 10 min at each pH before conductance was measured. The pH of the cis compartment was then adjusted with unbuffered 100 mM dimethylglutaric acid. Little activity is seen above pH 6, whereas activity increased below pH 6. This increase continued to at least pH 4.

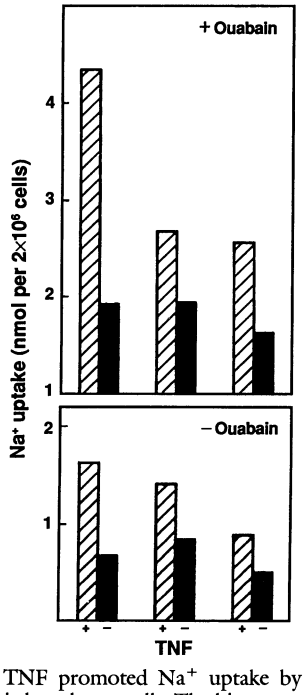

Fig. 3. TNF promoted Na^+ uptake by human histiocytic lymphoma cells. The histograms depict the amount of Na^+ taken up by TNF-treated (hatched bars) and untreated (solid bars) U937 cells. Three independent experiments are shown for uptake studies conducted in the presence and absence of ouabain (*31*).

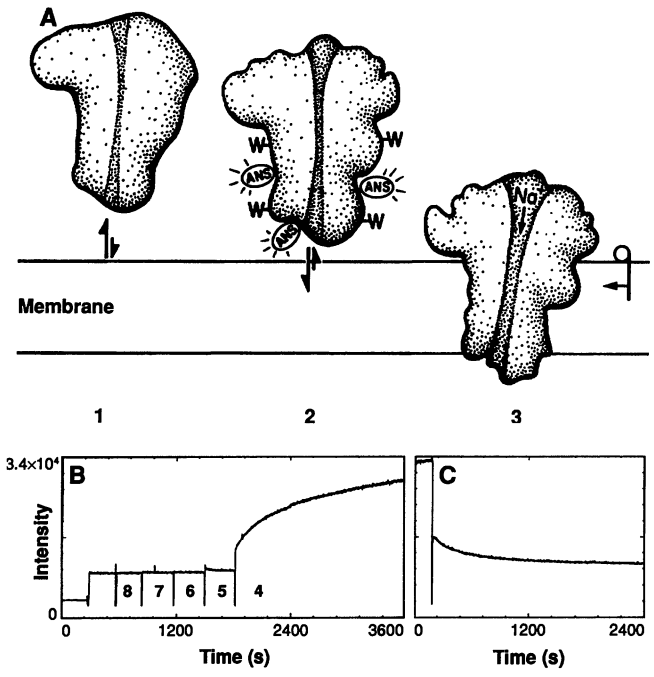

Fig. 4. (**A**) A model for TNF-membrane interactions and channel formation. Step 1, transient interaction of TNF with the membrane bilayer [which includes insertion at pH 7, although to a lower extent than at acid pH (*6, 9*)]. Step 2, acid-induced [and perhaps receptor-induced (*8*)] conformational changes lead to acquisition of ANS binding sites [see (B) and (C)] and exposure of tryptophan (W) residues (*9*). Step 3, membrane penetration by TNF molecules that have undergone appropriate hydrophilic to hydrophobic transitions in conformation (*6, 9*). Membrane insertion in the presence of Na^+ enables the TNF trimer to express channel activity. A photoreactive glycolipid probe (*6, 9*) is shown on the right. (**B**) TNF acquires hydrophobic binding sites at low pH. The fluorescence intensity of ANS is plotted against time at the indicated pH (*27*). The units of fluorescence are arbitrary. Dips in fluorescence intensity are caused by closing the shutter [and reflect the sequential addition to pH 8 buffer (*27*) of ANS, TNF, and 1 N HCl]. (**C**) Reversibility of the acid-induced conformational change of TNF. The fluorescence intensity of ANS (*32*) is shown to decrease abruptly upon returning the pH of the TNF sample to 8 after 30 min at pH 4.

ists in the neighborhood of cells that secrete TNF.

Our model for TNF channel formation (Fig. 4A) takes into account data from intramembranous photolabeling studies (*6*) and from studies in which we monitored the effects of low pH on TNF conformation. The compound 8-anilino-1-naphthalenesulfonic acid (ANS) has been widely used both as a probe of hydrophobic binding sites and as a highly sensitive detector of protein structural alterations (*17, 18*). A small amount of ANS-TNF association occurred at pH 5 (Fig. 4B). Lowering the pH to 4 provoked a rapid conversion in TNF structure and then a relatively slower conversion event. The biphasic nature of this conformational change mimicked the progression from membrane binding to intramembranous insertion observed in experiments with TNF and lipid vesicle targets (*9*). The blue shift in the ANS fluorescence maximum after association with TNF at low pH (*9*) reflects acquisition of a hydrophobic binding pocket for ANS (*18*). TNF rapidly lost the ability to bind ANS when the pH was returned to 8, thereby demonstrating full reversion to a hydrophilic configuration (Fig. 4C).

Further evidence for acquisition of hydrophobic properties at low pH is the dramatic decrease in the intrinsic fluorescence of TNF at low pH, indicating that its tryptophan residues (two per monomer; W in Fig. 4A) have become exposed to the surface (*9*). TNF is a trimer in solution (*7, 19*). The observation that vesicle-bound TNF is more susceptible to digestion by endoproteinase argC than is unbound TNF (*9*) indicates that the membrane-bound TNF conformer is somewhat different from the soluble TNF conformer. Recent cross-linking studies have revealed that regardless of whether TNF is bound to fluid or frozen lipid vesicles, it retains its trimeric structure. Intramembranous photolabeling of the trimer has also been demonstrated (*9*). Therefore, the plasticity of the TNF trimer may allow for channel opening and closing but does not appear to be sufficient for trimer disassembly. Relevant to these findings is the report that a long-lived cellular pool of internalized TNF appears to be membrane-integrated (*20*). Taken together, these findings support our proposal that at least one functional form of TNF is a membrane-embedded trimer, the effects of which are mediated through its ion channel–forming activity. Indeed, such an activity could well provoke responses specific to cell type, with membrane depolarization and altered free Na^+ levels being handled according to each cell's unique transporter composition and ion-modulated enzyme systems.

The three-dimensional structure of TNF is similar to that of several viral coat proteins (*4*), including the influenza hemagglutinin HA, which has membrane fusogenic activity that is dependent on pH. This suggests a possible role for the "jelly roll" motif in facilitating acid-dependent membrane penetration. Our results also raise the possibility that acid-facilitated conformational changes and subsequent membrane penetration may allow the central pore-like region of the TNF trimer to assume an "open" state.

Qualitative agreement between our cellular and planar bilayer findings suggests that channel activity may be physiologically relevant. Channel formation by TNF would explain the rapid decrease in resting membrane potential in skeletal muscle (*11*), the increased cellular Na^+ and water levels of endotoxic shock (*12*), and myelin dilatation, oligodendrocyte necrosis, and periaxonal swelling (*13*). The presence of TNF-specific receptors on the plasma membrane (*21*) might compensate for the relatively low channel-forming activity of TNF seen with planar membranes at neutral pH [for example, by facilitation of membrane insertion (*8*)]. Localized acid effects are also possible both intracellularly (for example, in endosomes) and extracellularly [for example, near activated macrophages and osteoclasts (*16*)]. Acidification of TNF decreased specific binding to U937 cancer cells, but it enhanced the killing activity (*6, 8, 9*). The pH dependence of channel formation may account for the ability of TNF to exert disparate cytotoxic and hormonal actions.

Development of specific channel blockers and enhancers for the TNF ion channel may enable clinicians to control the deleterious effects of TNF (for example, septic shock) and to augment the therapeutic ones (for example, cancer cell destruction). In this regard it should be noted that amiloride analogs were recently shown to inhibit TNF killing of murine L929 and L-M(TK^-) cells through an effect not related to blocking of the Na^+-H^+ antiporter (*22*).

REFERENCES AND NOTES

1. B. Beutler and A. Cerami, *Annu. Rev. Biochem.* **57**, 505 (1988); *Annu. Rev. Immunol.* **7**, 625 (1989); C. Q. Earl, J. M. Stadel, M. A. Anzano, *J. Biol. Response Modif.* **9**, 361 (1990); L. F. Fajardo and G. E. Grau, *West. J. Med.* **154**, 88 (1991).
2. L. Osborn, S. Kunkel, G. J. Nabel, *Proc. Natl. Acad. Sci. U.S.A.* **86**, 2336 (1989).
3. S. M. Russel, K. G. Krquer, I. F. C. McKenzie, G. A. Pietersz, *Cancer Res.* **50**, 6028 (1990).
4. E. Y. Jones, D. I. Stuart, N. P. C. Walker, *Nature* **338**, 225 (1989).
5. M. J. Eck and S. R. Sprang, *J. Biol. Chem.* **264**, 17595 (1989); S. R. Sprang and M. J. Eck, in *Current Research in Protein Chemistry: Techniques, Structure, and Function*, J. J. Villafranca, Ed. (Academic Press, New York, 1990), chap. 35.
6. R. L. Baldwin *et al.*, *J. Immunol.* **141**, 2352 (1988).
7. R. A. Smith and C. Baglioni, *J. Biol. Chem.* **262**, 6951 (1987).
8. M. P. Chang and B. J. Wisnieski, *Infect. Immun.* **58**, 2644 (1990); unpublished observations.
9. R. L. Baldwin, thesis, University of California, Los Angeles (1990).
10. N. Oku *et al.*, *J. Biochem. (Tokyo)* **102**, 1303

(1987); T. Yoshimura and S. Sone, *J. Biol. Chem.* **262**, 4597 (1987).
11. K. J. Tracey *et al.*, *J. Exp. Med.* **164**, 1368 (1986).
12. J. N. Cunningham, Jr., N. W. Carter, F. C. Rector, Jr., D. W. Seldin, *J. Clin. Invest.* **50**, 49 (1971).
13. K. W. Selmaj and C. S. Raine, *Ann. Neurol.* **23**, 339 (1988).
14. B. L. Kagan, M. Colombini, A. Finkelstein, *Proc. Natl. Acad. Sci. U.S.A.* **78**, 4950 (1981); J. J. Donovan, M. I. Simon, R. K. Draper, M. Montal, *ibid.*, p. 172; D. H. Hoch *et al.*, *ibid.* **82**, 1692 (1985).
15. J. D.-E. Young, *Immunol. Lett.* **19**, 287 (1988).
16. I. A. Silver, R. J. Murrills, D. J. Etherington, *Exp. Cell Res.* **175**, 266 (1988).
17. L. Stryer, *J. Mol. Biol.* **13**, 482 (1965); J. D. Johnson, M. A. El-Bayoumi, L. D. Weber, A. Tulinsky, *Biochemistry* **18**, 1292 (1979).
18. J. Slavick, *Biochim. Biophys. Acta* **694**, 1 (1982).
19. P. Wingfield, R. H. Paine, S. Craig, *FEBS Lett.* **211**, 179 (1987).
20. F. C. Kull, Jr., and J. M. Besterman, *J. Cell. Biochem.* **42**, 1 (1990).
21. H. Loetscher *et al.*, *Cell* **61**, 351 (1990); T. J. Schall *et al.*, *ibid.*, p. 361; C. A. Smith *et al.*, *Science* **248**, 1019 (1990).
22. B. Vanhaesebroeck *et al.*, *FEBS Lett.* **261**, 329 (1990).
23. M. Montal, *Methods Enzymol.* **32**, 545 (1974); B. L. Kagan, M. E. Selsted, T. Ganz, R. I. Lehrer, *Proc. Natl. Acad. Sci. U.S.A.* **87**, 210 (1990).
24. Y. Kagawa and E. Racker, *J. Biol. Chem.* **246**, 5477 (1971).
25. The membranes were composed of asolectin, and the aqueous phases were 100 mM NaCl, 5 mM dimethylglutarate acid, 2 mM $MgCl_2$, and 1 mM EDTA. The pH was 6.8 in the cis compartment and 7.2 in the trans compartment. TNF was added to a final concentration of 12.5 ng/ml.
26. J. B. Smith and E. Rozengurt, *Proc. Natl. Acad. Sci. U.S.A.* **75**, 5560 (1978).
27. R. M. C. Dawson, D. C. Elliott, W. H. Elliott, K. M. Jones, Eds., *Data for Biochemical Research* (Oxford Univ. Press, London, ed. 2, 1969), p. 501. Stocks (1 M) were prepared and diluted to 0.15 M.
28. "Solvent-free" membranes were prepared as described (*23*) with squalene (Sigma) or squalane (Fluka) to coat a hole (100 to 200 μm in diameter) in a Teflon partition. Monolayers were spread from mixtures of soybean phosphatidylethanolamine (40%), soybean phosphatidylcholine (40%), and bovine phosphatidylserine (20%) (Avanti, Pelham, AL). Occasionally this lipid mixture was mixed 1:1 with asolectin (*24*). Capacitance measurements were used to monitor bilayer formation from the apposition of the two monolayers. After membrane formation, the conductance ($g = I/V$) of the unmodified membrane was ohmic and was ~5 to 10 pS. All membranes used exhibited low conductance and were stable to voltages of ±100 mV for at least 10 min before the addition of TNF. The aqueous phases usually included 100 mM NaCl, 5 mM dimethylglutaric acid (pH 4.5) or 5 mM tris (pH 7.2) as buffer, 2 mM $MgCl_2$, and 1 mM EDTA. Voltage-clamp conditions were used; a battery-driven stimulator was used to apply voltages and a Keithley 427 current amplifier was used to measure current, which was recorded on an oscilloscope and a chart recorder. The cis compartment, to which TNF was added, is defined as ground. Voltages refer to the trans compartment, opposite the TNF-containing side and analogous to the cytosol of a target cell. In ion-selectivity experiments, salt gradients were imposed across the membrane, and the zero-current reversal potential E, where $I = g(V - E)$, was measured. Silver/silver chloride electrodes were used to connect the solutions to the electronics, and 3 M KCl/agar salt bridges were used in salt gradient experiments. Human recombinant (clinical grade) TNF was from Genentech (South San Francisco, CA); similar results were obtained with natural TNF from Calbiochem (San Diego, CA).
29. Same buffer as in Fig. 2A [see (*25*)], but pH 7.2 cis, pH 7.2 trans, and +100 mV. The lipid was a mixture of asolectin (33%), soybean phosphatidylethanolamine (27%), soybean phosphatidylcholine (27%), and bovine phosphatidylserine (13%); final concentration of TNF was 100 ng/ml.
30. Data are from a single membrane composed of 40% soybean phosphatidylethanolamine, 40% soybean phosphatidylcholine, and 20% bovine phosphatidylserine. The aqueous phase, containing 100 mM NaCl, 5 mM tris (pH 7.2 initially), 2 mM $MgCl_2$, and 1 mM EDTA, was continuously stirred. The final concentration of TNF was 400 ng/ml.
31. Human U937 cells (American Type Culture Collection, ATCC) were washed four times in buffer A (100 mM choline chloride, 25 mM $MgCl_2$, 5 mM KCl, and 20 mM Hepes, with the addition of 7.17 mM NaOH to adjust the pH to 7.2). Each sample, containing 2×10^6 cells, was resuspended in 200 μl of buffer A after the last wash and equilibrated at 4°C for 15 min before the addition of 1 μg TNF (2 μl of a 0.5 mg/ml stock in 10 mM sodium phosphate and 0.2 M NaCl; pH 7) or 2 μl of buffer alone. Binding was allowed to proceed for 2 hours at 4°C. Then 10 μl of 20 mM ouabain in water or 10 μl of water alone were added, and the samples were incubated for 13 min at 37°C. Next, 10 μl of $^{22}NaCl$ [10 μM stock, 200 μCi/ml (Amersham, Arlington Heights, IL)] were added to each sample, and incubation at 37°C was continued for 10 min. Ice-cold PBS (0.8 ml; 10 mM sodium phosphate and 150 mM NaCl) was added to stop the flux of $^{22}Na^+$. The cells were pelleted in a microcentrifuge (Beckman) and washed twice with 1 ml of PBS. Aliquots (10 μl) of the first and last supernatants were removed for counting. Pelleted cells were solubilized by incubation for 15 min with 100 μl of 0.5% Triton X-100 in buffer A at 37°C. Solubilized cells and supernatant aliquots were mixed with 10 ml of liquid scintillant and counted at the ^{14}C setting of a Beckman scintillation counter. Na^+ uptake values are based on the presence of 9.365 mM Na^+ (radioactive plus cold). This assay is a modification of that of Smith and Rozengurt (*26*).
32. Fluorescence measurements were performed with a SPEX Fluorolog II spectrophotometer. In all studies, slit widths were 1.25 mm (band pass of 2.25 nm), the samples were stirred at 37°C, and the fluorescence measurements were taken in the ratio mode. The pH was adjusted by the addition of 1 N HCl or NaOH (<1% total volume) and monitored with a microelectrode. ANS (Eastman Kodak, Rochester, NY) binding studies were performed with 2 ml of buffer [0.15 M sodium citrate-phosphate-chloride, pH 8 initially (*27*)] having 4 μM of ANS and 10 μg of TNF. The graphs in Fig. 4, B and C, represent a single time scan with excitation and emission wavelengths of 380 nm and 480 nm, respectively. ANS was freshly prepared in the buffer. The quantum yield of fluorescence is dependent on environmental polarity (*17*) and is insensitive to pH over a wide range (*18*).
33. We are grateful to Genentech for supplying us with human recombinant TNF, to L. Greene for expert technical assistance, and to G. Eisenman and other colleagues for valuable comments. This work was supported by the Department of Veterans Affairs and National Institute of Mental Health grant MH43433 (B.L.K.) and by NIH grant GM22240 (B.J.W.). R.L.B. held an NIH Atherosclerosis Predoctoral Training Grant Award (2 T32 HL07386).

25 October 1991; accepted 16 January 1992

Identification of a Major Growth Factor for AIDS–Kaposi's Sarcoma Cells as Oncostatin M

BALA CHANDRAN NAIR, ANTHONY L. DEVICO, SHUJI NAKAMURA,* TERRY D. COPELAND, YING CHEN, ATUL PATEL, TREVOR O'NEIL, STEPHEN OROSZLAN, ROBERT C. GALLO, M. G. SARNGADHARAN†

Conditioned medium from human T cell leukemia virus type 2 (HTLV-II)–infected T cells supports the growth and long-term culture of cells derived from acquired immunodeficiency syndrome (AIDS)–associated Kaposi's sarcoma lesions (AIDS-KS cells). A protein of 30 kilodaltons was purified from conditioned medium that supports the growth of AIDS-KS cells. The amino-terminal sequence of this protein was identical to the amino-terminal sequence of Oncostatin M, a glycoprotein that inhibits the growth of a variety of cancer cells. Oncostatin M from conditioned medium stimulated a twofold increase in the growth of AIDS-KS cells at a concentration of less than 1 nanogram of the protein per milliliter of medium.

KAPOSI'S SARCOMA (KS) IS A MULTICENTRIC NEOPLASM found predominantly in males and frequently associated with human immunodeficiency virus (HIV) infection (*1, 2*). The KS lesion has a complex histology characterized by the proliferation of spindlelike cells with neovascularization. These lesions are often infiltrated by inflammatory cells, fibroblasts, and endothelial cells (*2, 3*). The mechanism underlying the pathogenesis of this complex tumor is not clearly understood.

Several cytokines, including interleukin-1, interleukin-6, and tumor necrosis factor–α, induce the growth of cells derived from AIDS-KS cells (*4–6*). These cells are morphologically similar to the spindlelike cells observed in KS lesions (*7*). The HIV-1 Tat protein has also been shown to enhance the growth of AIDS-KS cells at very low concentrations (*8*).

B. C. Nair, A. L. DeVico, Y. Chen, A. Patel, T. O'Neil, M. G. Sarngadharan, Department of Cell Biology, Advanced BioScience Laboratories, Inc., Kensington, MD 20895.
S. Nakamura and R. C. Gallo, Laboratory of Tumor Cell Biology, National Cancer Institute, National Institutes of Health, Bethesda, MD 20892.
T. D. Copeland and S. Oroszlan, Laboratory of Molecular Virology and Carcinogenesis, Advanced BioScience Laboratories–Basic Research Program, National Cancer Institute–Frederick Cancer Research and Development Center, Frederick, MD 21702.

*Present address: Department of Internal Medicine, University of Southern California, Los Angeles, CA 90033, and Huntington Memorial Hospital, Los Angeles, CA 91105.
†To whom correspondence should be addressed.